Cell-surface phenotyping identifies CD36 and CD97 as novel markers of fibroblast quiescence in lung fibrosis

Katharina Heinzelmann[1]*, Mareike Lehmann[1], Michael Gerckens[1], Nina Noskovičová[1], Marion Frankenberger[1], Michael Lindner[1,2], Rudolf Hatz[2,3], Jürgen Behr[2,4], Anne Hilgendorff[1,5,6], Melanie Königshoff[1,7], and Oliver Eickelberg[1,7]*

* Katharina Heinzelmann and Oliver Eickelberg contributed equally to this work.

[1]Comprehensive Pneumology Center, University Hospital of the Ludwig-Maximilians University (LMU) Munich and Helmholtz Zentrum München, Member of the CPC-M BioArchive, Member of the German Center for Lung Research (DZL), Munich, Germany

[2]Thoraxchirurgisches Zentrum München, Asklepios Fachkliniken München-Gauting, Munich, Germany

[3]Thoraxchirurgisches Zentrum, Klinik für Allgemeine-, Viszeral-, Transplantations-, Gefäß- und Thoraxchirurgie, Klinikum Großhadern, Ludwig-Maximilians-Universität (LMU), Munich, Germany

[4]Medizinische Klinik und Poliklinik V, Klinikum der Ludwig-Maximilians-Universität (LMU), Munich, Germany

[5]Department of Neonatology, Perinatal Center Grosshadern, Ludwig-Maximilians University (LMU), Munich, Germany

[6]Center for Comprehensive Developmental Care, Dr. von Haunersches Children's Hospital University Hospital Ludwig-Maximilians University (LMU), Munich, Germany

[7]Division of Respiratory Sciences and Critical Care Medicine, University of Colorado, Denver, CO, USA

Running head: Cell-surface profiling in human lung fibroblasts

Author's contributions:

Conception and design: KH, ML, NN, MK, and OE

Analysis and interpretation: KH, ML, MG, NN, MF, ML, RH, JB, AH, MK, and OE

Drafting the manuscript for important intellectual content: KH, ML, MG, NN, AH, MK, and OE

To whom correspondence should be addressed:

Oliver Eickelberg, Division of Respiratory Sciences and Critical Care Medicine,

University of Colorado, Denver, CO, USA

Email: oliver.eickelberg@ucdenver.edu

Phone: (303)724-4075, Fax: (303)724-6042

Keywords

Cell culture, surface marker, mesenchymal marker, FACS, replicative senescence, IPF.

Glossary

TGF-β	transforming growth factor-beta
ECM	extracellular matrix
αSMA	alpha-smooth muscle actin
MSC	mesenchymal stromal cells

Abstract

Fibroblasts play an important role in lung homeostasis and disease. In lung fibrosis, fibroblasts adopt a proliferative and migratory phenotype, with increased expression of α-smooth muscle actin (αSMA) and enhanced secretion of extracellular matrix components. Comprehensive profiling of fibroblast heterogeneity is limited, due to a lack of specific cell-surface markers. We have previously profiled the surface proteome of primary human lung fibroblasts.

Here, we sought to define and quantify a panel of cluster of differentiation markers in primary human lung fibroblasts and IPF lung tissue, using immunofluorescence and FACS analysis. Fibroblast function was assessed by analysis of replicative senescence.

We observed presence of distinct fibroblast phenotypes *in vivo*, characterized by various combinations of Desmin, αSMA, CD36, or CD97 expression. Most markers demonstrated stable expression over passages *in vitro*, but significant changes were observed for CD36, CD54, CD82, CD106, and CD140a. Replicative senescence of fibroblasts was observed from passage 10 onward. CD36- and CD97-positive, but αSMA-negative, cells were present in remodeled areas of IPF lungs. Transforming growth factor-β treatment induced αSMA and collagen I expression, but repressed CD36- and CD97 expression.

We identified a panel of stable surface markers in human lung fibroblasts, applicable for positive cell isolation directly from lung tissue. TGF-β exposure represses CD36- and CD97 expression, while increasing αSMA expression; we therefore identified complex surface protein changes during fibroblast-myofibroblast activation. Co-existence of quiescence and activated fibroblast subtypes in the IPF lung suggests dynamic remodeling of fibroblast activation upon subtle changes to growth factor exposure in local microenvironmental niches.

Introduction

Fibroblasts represent the main extracellular matrix (ECM)-producing cell type in the lung. Several growth factors, such as transforming growth factor-β (TGF-β), Wnt-5A, and sonic hedgehog, are known to activate fibroblasts into myofibroblasts - a highly proliferating and migrating phenotype characterized by α-smooth muscle actin (αSMA) expression and enhanced secretion of ECM components (8, 20, 25, 27, 28, 50, 52). Myofibroblasts participate in wound healing, but are also associated with tissue fibrosis in several organs, including the lung. A number of different cell types have been shown to give rise to myofibroblasts, including fibrocytes, pericytes, mesenchymal stromal cells (MSC), alveolar epithelial type II cells, or endothelial cells (13, 20). This is also reflected in the expression of fibroblast markers, e.g. αSMA, CD90/Thy-1, most of which are also expressed in other cell types, e.g. smooth muscle cells, endothelial cells, epithelial cells, or mesenchymal stromal cells (2, 14, 24). To date, specific cell-surface markers that identify a distinct population of fibroblasts remain to be defined. The classical markers associated with fibroblasts in disease are intracellular markers (e.g. αSMA) or secreted proteins (e.g. fibronectin, collagen type I), and accordingly, are not suitable for cell-specific isolation by FACS. In addition, few studies have analyzed surface marker expression in fibroblasts in different organs or species (1, 17, 31, 38, 47). CD9, CD90, CD106, CD166, or ITGA11 are expressed exclusively on fibroblasts compared with MSC, fibrocytes, monocytes, or macrophages. In the mouse, Sca-1 and CD49e seem to be differentially expressed between fibroblasts and myofibroblasts. Therefore, the presence of fibroblast subtypes in healthy tissue, in particular in the lung, their characteristic marker expression, as well as their contribution to disease, remains unclear.

Fibroblasts play a crucial role in several chronic lung diseases. Idiopathic pulmonary fibrosis (IPF) is characterized by excessive tissue remodeling and scaring, with increased ECM deposition by activated fibroblasts. Many developmental pathways, such as Wnt and sonic hedgehog (9, 34), are reactivated in IPF cells, due to the release of profibrotic mediators, such as PDGF and CTGF, and by autocrine and paracrine mechanisms (22, 32, 52, 53). In addition, several novel mediators of myofibroblast activation have recently been described, such as FKBP10 or Sirtuin 7, both of which mediate expression of αSMA and collagens (57,

65). Also, fibrotic myofibroblasts are more resistant to apoptosis due to Thy-1 interaction with FAS and endothelin-1 induced expression of survivin (21, 36).

The standard technique for fibroblast isolation is by cell outgrowth from tissue pieces (56, 58, 59, 61). Primary fibroblasts can be kept in cell culture for several passages, still susceptible for cytokine stimulation and other cellular treatments. Therefore, cultured primary fibroblasts represent a common model to simulate fibrotic conditions *in vitro* and to study fibroblasts and their cellular mechanisms taking part in lung fibrosis (15, 23, 32, 43, 49, 65). Their phenotype, functionality and potential expression changes of markers over time under standardized culture conditions, however, has not been characterized in detail (5).

The aim of our study was to gain insight into potential fibroblast subtypes by analyzing surface and intracellular protein expression in primary human lung fibroblasts, as well as assess fibroblast protein expression and function over time using primary cultures from passages 1 through 12. Based on our recently published surface proteome analysis of primary human lung fibroblasts (19), in which we also identified proteins regulated by TGF-β, we selected a panel of cluster of differentiation (CD) markers and determined their expression, as well as those of the classical markers CD90/Thy-1, αSMA, fibronectin, collagen type I, or Desmin. We further determined expression changes over time in culture, after stimulation with TGF-β, and defined the onset of senescence in fibroblast cultures. We determined the cellular localization and expression of the markers CD36, CD97, and Desmin together with αSMA in IPF tissue versus control. Most of the analyzed markers are consistently expressed over time in different passages, but a significant change of % positive cells was observed for CD36, CD54, CD82, CD106, and PDGFRα (CD140a). Fibroblasts turned senescent from passage 10 on, which correlated with highest number of positive cells for the markers CD36 and CD82. Further, CD36 and CD97 were increasingly detectable in remodeled regions of IPF tissue compared with control, but negative for αSMA. These data point to the existence of (non-activated) fibroblast subtypes and will help to define and isolate distinct subpopulations by their surface marker expression for further characterization in disease. Further, we provide detailed information about the functionality and phenotypic characteristics of primary human fibroblasts, which are widely used in the community as *in vitro* models for mechanistic studies of cells in fibrosis.

Materials and Methods

Cell culture and treatments

Primary human lung fibroblasts were isolated from human lung tissue derived from tumor-free areas of lung resections, from tissue donors or from explants after transplantation, as described in the respective legends. The study was approved by the local ethics committee of the LMU München (333-10, removal-request 454-12). Diagnosis of IPF was made by multidisciplinary consensus, based on the current criteria of the American Thoracic Society and European Respiratory Society (48). Cells were isolated as described previously (57), taken in culture and used for experiments in different passages as indicated. Cells were cultured in Dulbecco's modified Eagle medium/F12 supplemented with 20% fetal bovine serum (FBS) and 100 U/ml Penicilline/Streptomycin and split with 0.25Trypsin/EDTA in a ratio of 1:5 when confluency of 80% was reached, if not indicated different. Purity of fibroblasts was determined by CD45-/CD31-negative and CD90-positive expression between passage 1 and 7 using FACS and qPCR, and a pure population (negative for CD45 and CD31) detected from passage 2 on (data not shown). TGF-β1 treatment was performed as described previously (19).

Immunofluorescent stainings of primary fibroblasts

Cells were seeded in a 96-well plate (8000 cells per well) and incubated for 24 hours at 37°C in an atmosphere of 5% CO_2. Cells were washed with PBS, fixed with 4% PFA for 15 min at RT, washed again, and blocked in 5% BSA for 30 min. For intracellular antibody staining, cells were permeabilized with 0.25% Triton X-100 for 15 min. Primary and secondary antibody incubation was performed in antibody diluent (Zytomed) for 60 and 45 min at room temperature, respectively. Used antibodies are listed in Table 1. Cells were again washed, fixed with 4% PFA for 15 min, washed and left in PBS at 4°C. Images were acquired using a laser scanning confocal microscope (LSM) 710 (Zeiss) and Zen software. Quantification of total cells was performed by using Imaris software. The number of positive cells was assessed by independent counting of two scientists.

Immunofluorescent stainings of paraffin embedded lung sections

Paraffin embedded lung sections of 200 µm were deparaffinized as described previously (57). Heat-mediated antigen retrieval was performed by using R-universal buffer and Retriever 2100 (BioVendor, Germany). Sections were blocked in 5% BSA for 40 min and stained with primary antibodies diluted in antibody diluent (Zytomed Systems, Germany) overnight at 4°C. After washing, lung sections were incubated with fluorochrome conjugated secondary antibodies for 1 hour, washed again and stained with DAPI for 7 min. Slides were covered with Dako Fluorescence Mounting Medium (Agilent Technologies, Germany) and stored at 4°C. Images were acquired using an Axio Imager M2 (Zeiss, Germany). For control stainings, a secondary antibody staining alone was performed with same patient derived lung sections and images acquired using the same exposure time and display settings (data not shown).

FACS analysis

Surface staining was performed as described previously (19). Blocking was performed with Human TruStain FcX™ (Biolegend). For intracellular stainings, cells were fixed and permeabilized with Cytofix/Cytoperm, washed with 1 x Perm/Wash buffer (Cytofix/Cytoperm™ Kit, BD) and stained with antibodies for 25 min at 4°. Cells were washed twice with 1 x Perm/Wash buffer followed by an Alexa Fluor 488-conjugated secondary antibody staining for 15 min at 4°, and again washed with 1 x Perm/Wash buffer. Stained cells were fixed with 4% PFA for 15 min at RT, washed again and resuspended in FACS buffer. All antibodies are listed in Table 1. Stained cells were measured with a FACS LSRII (BD). Data were analyzed with FlowJo software version 9.6.4. Number of positive cells was determined in comparison to isotype controls set as negative. Crossing point of population curves was determined and the percentage of isotype subtracted. Fluorescence intensity was calculated by total median values of positive staining minus total median values of corresponding isotype controls.

Cells from Figure 2 and 4 were simultaneously triggered with TGF-β, and these FACS data are shown in figure 7.

SDS-PAGE and Western immunoblotting

Total protein lysates were extracted with RIPA-buffer (50 mM Tris·HCl, pH 7.6, 150 mM NaCl, 1% Nonidet P-40, 0.5% sodium deoxycholate, and 0.1% SDS) supplemented with CompleteTM protease inhibitor cocktail (Roche) and PhosSTOP phosphatase inhibitor cocktail (Roche). Protein concentration was determined with a BCA assay (Pierce), and 25 µg of whole cell lysate were loaded on 17% polyacrylamide gels, separated, and detected by WB as previously described (39). Used antibodies are listed in Table 1.

Beta-galactosidase assay

40000 cells were seeded in 6-well plates. After 24 hours, medium was changed to medium containing 5% FBS. After additional 72 hours cells were counted or stained for senescence-associated (SA) -β-galactosidase (Senescence β-Galactosidase Staining Kit, Cell Signaling Technology) according to manufacturer´s instructions. Images were acquired using a Zeiss Axiovert 40C microscope (100x magnification). Counting of blue cells and total cells of three independent areas of each well (a minimum of 60 cells) was performed to determine the percentage of senescent cells.

Flow cytometry based detection of SA- beta-Galactosidase

Detection of SA-beta galactosidase by FACS was performed as described previously (11, 35). Briefly, fibroblasts were seeded on 10 cm dishes in passage 9 or 10, grown confluent and incubated with bafilomycin A1 (100 nm, Enzo Life Sciences) in 5 ml fresh medium for 1 h and further C_{12}FDG (33 µM) added for 2h. Cells were washed twice with PBS, trypsinized and FACS staining of surface markers CD36 and CD97 performed as described above.

IL-6 ELISA

40000 cells were seeded in 6-well plates. After 24 hours, medium was changed to medium containing 5% FBS. After additional 72 hours supernatants were taken and centrifuged at 14000 g for 10 min at 4°C. Samples were stored at -80°C before being transferred to the ELISA plate and the assay was performed according to the manufacturer's instructions (DY206-05; R&D, Minneapolis, Minnesota, USA). Values were normalized to respective cell numbers after 72h.

Graphical data representation and statistical analysis

GraphPad Prism 5 was used for graphical representation of data and statistical analysis (details indicated in figure legends).

Results

Mesenchymal marker expression in primary human lung fibroblasts. Several markers, such as fibronectin (FN) or alpha-smooth muscle actin (αSMA), have been commonly used to characterize a (myo)fibroblast phenotype. We first analyzed the expression pattern and the number of positive cells for the markers collagen type I (Coll I), FN, αSMA, Desmin and CD90/Thy-1. Immunofluorescent stainings showed that the majority of cells expressed Coll I, FN and CD90/Thy-1 (93 ± 4%, 98 ± 2.5%, 99 ± 1.5%), whereas only single cells were stained positive for αSMA and Desmin (3 ± 2.2%, 5 ± 0.02%) (Fig. 1A,C). In double stainings, two subtypes of Desmin- positive fibroblasts were detected, either single positive for Desmin or also double-positive for αSMA (4.4 ± 3.8% versus 3.5 ± 3.8%) (Fig. 1B,D). Mesenchymal marker expression was again analyzed and quantified by the unbiased technique of FACS analysis (Fig. 2A,B) identifying all cells highly positive for CD90/Thy-1 (94 ± 3.2%). The other markers spread in the number of positive cells between patients, the majority, however, still positive for Coll I and FN (66 ± 12.9%, 53 ± 15.8%) but less for Desmin (44 ± 8.5%).

Surface marker detection in primary lung fibroblasts. In our recently described lung fibroblast surface proteome (19), we identified proteins present on the surface of primary lung fibroblasts, a subgroup to be regulated by TGF-β. Based on this dataset, we selected the family of tetraspanins (CD9, CD63, CD81, CD82, CD151) for further analysis over extended passages of lung fibroblasts. More than 85% of fibroblasts were positive for these markers, whereas MFI values revealed CD63 to be most abundant on the fibroblast surface (Fig. 3). Additional CD markers were categorized e.g. into the family of complement receptors (CD46, CD55, CD59), or have been associated to be expressed on mesenchymal stromal cells (MSC), such as CD44, CD73, and CD105. Among these, CD26, CD44, CD46, CD47, CD55, CD59, CD73, and CD105 were detectable in the majority of fibroblasts (more than 80%), whereas interestingly, CD36, CD54, CD97, and CD106 were just present in 7% (±6.9), 39% (±20.9), 22% (±22.2), and 23% (±15.7) of the cells, respectively. The percentage of cells positive for CD54, CD97 and CD106 spread widely between patients (Fig. 4A,B). Interestingly, CD26 and the MSC markers CD44, CD73 and CD105 seemed to be more abundant on the surface of fibroblasts than the other markers (Fig. 4C).

Changes of surface marker expression over time in culture. Next, we determined changes in the number of positive cells between different passages (passage 1-7) of cultured fibroblasts (Fig. 5). The markers CD9, CD44, CD46, CD55, CD59, CD63, CD73, CD81, CD90, CD105 and CD151 showed a consistent expression in more than 80% of the cells with no changes between early (p1) and late passages (p7) (Fig. 5B). Surface markers expressed in less than 80% and/or increasing/decreasing over time in culture are summarized in Figure 5C. Interestingly, CD36, CD82 and CD140a (PDGFRα) showed a significant increase of positive cells between passages, of which CD140a changed between passage 1 and 3 (11 ± 12.7% to 27 ± 9.4%), CD82 between passage 1 and 5 (75 ± 19.1% to 91 ± 3.3%) and CD36 between passage 1 and 7 (5 ± 8.3% to 32 ± 28.6%) (Fig. 5C). A strong decrease between passages was observed for the markers CD54 and CD106, starting with 76% (± 8.5) and 57% (± 10.8) positivity in passage 1, down to 25% (± 14.3) and 3% (± 4.4) in passage 7, respectively (Fig. 5C).

Functionality of fibroblasts in culture. First, we analyzed the time point of replicative senescence, a typical phenomenon of primary cells in culture. The β-galactosidase assay showed a significantly higher enzymatic activity from passage 10 onward (Fig. 6A,B), together with an increase of IL-6 secretion (Fig. 6C). IL-6 is a member of the senescence-associated secretory phenotype (SASP) and its secretion correlated with an increased doubling time of growing fibroblasts in culture from passage 10 onward (Fig. 6D). Further, the expression of the senescence associated cyclin-dependent kinase inhibitor P16 was slightly enhanced from passage 5 onward and strongly detected in passage 11 (Fig. 6E). Second, we activated fibroblasts by TGF-β stimulation to analyze the expression of selected markers in differentiated myofibroblasts by FACS (Fig. 7A). We depicted the intracellular mesenchymal reference markers collagen type I, fibronectin, and Desmin, and the surface markers CD36 and CD97, as indicated subtype markers. Interestingly, TGF-β significantly decreased the number of CD36- and CD97-positive cells, whereas fibronectin and collagen type I cells increased. No significant change was observed for Desmin. Next, we analyzed the senescent population, observed in higher passages, for CD36 and CD97 expression by FACS

(Fig. 7B). In the presence of C_{12}FDG, 91% (± 7.8) of total cells were determined senescent (Fig. 7C). 15.1% (± 9.3) and 22.3% (± 23) of cells were stained positive for CD36 and CD97, respectively, of which all intend to be part of the senescent population (Fig. 7D).

Subtype marker expression in human lung tissue. Next, we analyzed the *in vivo* relevance for some of the minor expressed (below 30% of total in fibroblasts) subtype markers. To do so, we stained human lung tissue sections of IPF and control with specific antibodies for CD36, CD97 and Desmin, as well as fibronectin and collagen type I as reference staining's. We detected positive cells for Desmin in control and remodeled areas of IPF tissue. A strong increase of positive cells for CD36 and especially CD97 was identified in remodeled IPF areas compared to control (Fig. 8). Interestingly, no co-staining with αSMA was detected for the markers CD36 or CD97, whereas single and double positive cells of Desmin were observed. Fibronectin and collagen type I, known reference markers being expressed and secreted by (myo)fibroblasts, mainly overlapped in expression with αSMA-positive cells, strongly increased in areas of stromal connective IPF tissue (Fig. 8).

Discussion

The lung fibroblast represents one of the most abundant cell types in the lung and contributes to significant ECM changes underlying wound healing and chronic lung disease. Primary fibroblasts have been isolated from lung tissue and used for *in vitro* studies simulating fibrosis conditions for decades. Despite this wide use, we lack comprehensive knowledge about their phenotypic characteristics, *in vivo* and *in vitro* heterogeneity, and specific functional responses under *in vitro* conditions. Thus, we sought to perform a comprehensive and detailed analysis of intracellular and surface marker heterogeneity of primary human lung fibroblasts *in vivo* in the human lung and *in vitro*. We studied expression changes during passaging *in vitro* and determined the time point of replicative senescence. Our data provide evidence for significant fibroblast heterogeneity within the whole population of lung fibroblasts, as defined by expression of αSMA, Desmin, CD36, CD97, or CD106. Moreover, we identified a panel of stable surface markers highly expressed in a number of fibroblasts from an early passage on, which can be used in future for marker-specific direct isolation of fibroblasts from human lung tissue.

A specific phenotype termed myofibroblasts has been a major focus, since activated fibroblasts turn into this αSMA-expressing and highly proliferative and migrating phenotype in their role as ECM-producing cells (20). The existence of other fibroblast subtypes, however, and their potential role in disease has not been clarified in sufficient detail in the human lung (1, 7, 46). Further, the distribution of classical mesenchymal markers, such as αSMA, fibronectin or collagen, in a population of fibroblasts has not been analyzed to date. Interestingly, among the majority of collagen type I positive fibroblasts in culture we observed two minor populations of cells, either single positive for Desmin or double positive for Desmin and αSMA. Intracellular markers, such as αSMA or Desmin, however, are not suitable for direct isolation by FACS, since this technique relies on cell surface proteins. Although limited, some data exist, describing surface marker expression in fibroblasts. In line with our results, CD44, CD73, CD90 and CD105 have been identified on fibroblasts. Their specificity, however, seems limited since MSC are also highly positive for those markers (2, 17, 31). We therefore used a broader panel of surface markers to unequivocally analyze the cell population present in the human fibroblast culture. Our study is confirmed by previous

studies, describing the expression of CD54, CD44 or CD81 (38, 47). Only one study has analyzed in detail lung fibroblasts, describing a panel of markers including CD44, CD73, CD90, CD105, CD9, CD29, and CD166, most of which we analyzed and detected as well (17). Our study exclusively gives a detailed insight in the expression patterns of primary lung fibroblasts, and the data will enable future FACS strategies for direct isolation of fibroblasts from human tissue.

It is feasible that the expression of specific markers *in vitro* might be the result of artificial changes that occur upon passaging steps and adherence to artificial material, and therefore may not reflect *in vivo* conditions. A study by Walmsley et al. compared surface marker expression of directly isolated dermal mouse fibroblasts with cells cultured for two weeks. They observed a shift in expression of several markers due to the culturing process, and reported an increase for e.g. CD54, CD140a, and CD81 (60). Similar observations were made by Halfon et al. The significant change in CD106, CD146, and CD9 expression in culture between passages 2 and 6 resulted in a loss of discriminating markers between MSC and fibroblasts derived from skin and lung (17). In our data, we confirmed an increase of CD140a and a decrease of CD54 and CD106 from low to high passages in culture, whereas no changes were detected for CD9 and CD81. One may, however, conclude from this data that markers changing within culture might probably not be suitable for cell type-specific isolation or phenotypic characterization in general. But these marker expression changes over passages might also have a functional consequence and gives an idea about sensitive markers potentially reflecting subcellular changes, e.g. cellular senescence. On the other hand, it illustrates the importance of identifying a panel of stable fibroblast (subtype) markers for FACS isolation from lung homogenate or in lower cell passages. This is strengthened by the fact that isolation of fibroblasts by negative selection remains difficult since main cell lineages of other mesenchymal cell types, such as smooth muscle cells, resident MSC, pericytes, or lipofibroblasts cannot be fully excluded from the fibroblast pool. In this study, we isolated cells by outgrowth from tissue, the most common and widely accepted technique in the field. We cannot exclude that other cell types transdifferentiated in culture into fibroblasts and contributed to the fibroblast pool analyzed. We will in future studies analyze the role of fibroblast subtype populations, such as CD36 and CD97 in disease, for which the origin of these cells must be clarified, but more in the context of identifying

and characterizing the cell type giving rise to the fibroblast in disease. This is supported in the literature by a number of recently published data studying mesenchymal populations and progenitors by lineage tracing or single-cell RNA sequencing in murine models, although future studies have to confirm the existence and relevance of such lineages in the human lung (12, 18, 30, 33, 51, 66).

We also tested the functionality of primary fibroblasts in culture and determined the onset of replicative senescence, a well-known effect occurring in primary cells in culture, and their ability to respond to cytokine stimulation (29). Replicative senescence of primary cells was detected from passage 8 to 10 onward. Therefore, it must be considered that phenotypic changes and experimental observations obtained from primary fibroblasts from approximately passage 8 onward might be due to replicative senescence of cells. We also report that the number of cells positive for CD36 and CD82 significantly increased in high passages. Both markers have been described to induce cellular senescence, thereby supporting these observations (6, 26, 37, 67). Further, TGF-β stimulation of primary fibroblasts led to a significant shift in surface marker expression. We detected increasing numbers of collagen type I- and fibronectin- positive cells, but observed a decrease of CD36- and CD97-positive cells.

We identified Desmin, αSMA, CD36, CD97, and CD106 to be expressed in a minor population of fibroblasts. To our knowledge, this has not been analyzed or observed before in other studies. Cells positive for these markers may present distinct subtypes of fibroblasts with unknown function in lung homeostasis and disease. In immunofluorescent stainings of IPF and control tissue, we observed few positive cells of potential mesenchymal background in control tissue, but with a strong increase of CD36 and CD97 expression in remodeled areas of IPF tissue, indicating a quiescent fibroblast background. In lung fibrosis, activated fibroblasts represent a highly proliferative, contractile and αSMA positive phenotype, accumulating in stromal connective tissue with increased secretion and deposition of ECM components (25, 40). Interestingly, CD36 and CD97 were not stained positive for αSMA, and thus are likely not activated fibroblasts. Further, TGF-β stimulation decreased the amount of CD36- and CD97-positive cells *in vitro*. Moreover, our *in vitro* data showed that all CD36 and CD97 positive cells are part of the senescent population in high passaged cells. To our knowledge, a potential role of CD97 in senescence has not been described before. We

therefore assume that the CD36- and/or CD97-positive population in dense fibrotic tissue does not represent a population of activated fibroblasts. The increase of this population in IPF tissue considers a potential role in disease, probably activated by a different stimulus. Senescence favors IPF and is associated with its pathology (3, 41, 55, 64). CD97 is a member of the G-protein coupled receptor family, with adhesive properties, known to be expressed on inflammatory, endothelial and smooth muscle cells, and bone marrow derived MSC. Functionally, CD97 is known to play a role in angiogenesis, tumor differentiation and invasion by interacting with its ligand CD55 (4, 42, 62). To our knowledge, no data exist connecting CD97 with fibrosis or the fibroblast phenotype. CD36, a multifunctional scavenger receptor is expressed on a variety of different cell types. Besides its potential role in cellular senescence, as discussed above, few other publications have described CD36 as a modulator of fibrotic processes in the lung (44, 45, 63). Silencing CD36 in macrophages in a silicosis rat model and a bleomycin mouse model resulted in inhibition of L-TGF-β1 activation and reduced numbers of αSMA-positive myofibroblasts, respectively. Future studies are needed to further characterize the impact of CD36 and CD97 on cellular senescence and to analyze the phenotype of fibroblast subtypes under physiological and pathophysiological conditions.

Our data indicate that subpopulations can be defined by marker expression and that surface markers may strongly be involved in cellular changes contributing to disease by multiple mechanisms. Although there is still a limitation in these studies, published data exist, clearly linking fibroblast surface proteins to fibrosis and as modulators of cell phenotypes. CD90/Thy-1, e.g., suppresses myofibroblast differentiation in healthy cells, but its expression is downregulated in IPF fibroblasts via an epigenetic mechanism of Thy-1 promotor methylation (10, 16, 54). Further, loss of CD90/Thy-1 leads to a profibrotic phenotype by TGF-β-induced MMP-9 expression (49). It is therefore important to further identify mesenchymal/fibroblast cell (sub)type markers in the future and to analyze their expression and function in the context of disease. Our detailed description of markers expressed in early and late passages will enable to better control phenotypic changes in culture and to identify the best time point for individually designed studies of fibroblast function in the context of disease. Further, our data intend that at least some phenotypic specific-

information is reflected in low passages of fibroblasts in culture under standardized conditions.

In sum, we identified a panel of stable surface markers in human lung fibroblasts, which can be used for positive cell isolation directly from lung tissue. CD36- and CD97-positive fibroblasts represent quiescent fibroblasts present in the control and IPF lung, which switch to αSMA-positive fibroblasts upon TGF-beta exposure. Co-existence of both fibroblasts subtypes in the IPF lung suggests dynamic remodeling of fibroblast activation upon subtle changes to growth factor exposure in local microenvironmental niches.

Acknowledgements

Human samples were kindly provided by the CPC-M BioArchive. We are grateful to Dibora Tibebu, Heike Hofmann, and Nadine Adam for excellent technical support, and Isis Fernandez and Gerald Burgstaller for valuable help and scientific discussions.

Grants

We thank the Helmholtz Association (BMBF) and the German Center for Lung Research (DZL) for funding this study.

Disclosures

Dr. Katharina Heinzelmann, Dr. Mareike Lehmann, Michael Gerckens, Nina Noskovičová, Dr. Marion Frankenberger, Dr. Michael Lindner, Dr. Rudolf Hatz, Dr. Jürgen Behr, Dr. Anne Hilgendorff, and Dr. Dr. Melanie Königshoff declare that they have no conflicts of interest with the contents of this article. Dr. Oliver Eickelberg reports personal fees from MorphoSys AG, Novartis Pharma AG, Galapagos NV, and Lanthio Pharma B.V., outside of submitted work.

References

1. **Akamatsu T, Arai Y, Kosugi I, Kawasaki H, Meguro S, Sakao M, Shibata K, Suda T, Chida K, and Iwashita T**. Direct isolation of myofibroblasts and fibroblasts from bleomycin-injured lungs reveals their functional similarities and differences. *Fibrogenesis Tissue Repair* 6: 15, 2013.
2. **Alt E, Yan Y, Gehmert S, Song YH, Altman A, Gehmert S, Vykoukal D, and Bai X**. Fibroblasts share mesenchymal phenotypes with stem cells, but lack their differentiation and colony-forming potential. *Biol Cell* 103: 197-208, 2011.
3. **Alvarez D, Cardenes N, Sellares J, Bueno M, Corey C, Hanumanthu VS, Peng Y, D'Cunha H, Sembrat J, Nouraie M, Shanker S, Caufield C, Shiva S, Armanios M, Mora AL, and Rojas M**. IPF lung fibroblasts have a senescent phenotype. *Am J Physiol Lung Cell Mol Physiol* 313: L1164-L1173, 2017.
4. **Aust G, Wandel E, Boltze C, Sittig D, Schutz A, Horn LC, and Wobus M**. Diversity of CD97 in smooth muscle cells. *Cell Tissue Res* 324: 139-147, 2006.
5. **Baglole CJ, Reddy SY, Pollock SJ, Feldon SE, Sime PJ, Smith TJ, and Phipps RP**. Isolation and phenotypic characterization of lung fibroblasts. *Methods Mol Med* 117: 115-127, 2005.
6. **Bandyopadhyay S, Zhan R, Chaudhuri A, Watabe M, Pai SK, Hirota S, Hosobe S, Tsukada T, Miura K, Takano Y, Saito K, Pauza ME, Hayashi S, Wang Y, Mohinta S, Mashimo T, Iiizumi M, Furuta E, and Watabe K**. Interaction of KAI1 on tumor cells with DARC on vascular endothelium leads to metastasis suppression. *Nat Med* 12: 933-938, 2006.
7. **Baum J, and Duffy HS**. Fibroblasts and myofibroblasts: what are we talking about? *J Cardiovasc Pharmacol* 57: 376-379, 2011.
8. **Bernard K, Logsdon NJ, Ravi S, Xie N, Persons BP, Rangarajan S, Zmijewski JW, Mitra K, Liu G, Darley-Usmar VM, and Thannickal VJ**. Metabolic Reprogramming Is Required for Myofibroblast Contractility and Differentiation. *J Biol Chem* 290: 25427-25438, 2015.
9. **Bolaños AL, Milla CM, Lira JC, Ramírez R, Checa M, Barrera L, García-Alvarez J, Carbajal V, Becerril C, and Gaxiola M**. Role of Sonic Hedgehog in idiopathic pulmonary fibrosis. *American Journal of Physiology-Lung Cellular and Molecular Physiology* 303: L978-L990, 2012.
10. **Bradley JE, Ramirez G, and Hagood JS**. Roles and regulation of Thy-1, a context-dependent modulator of cell phenotype. *Biofactors* 35: 258-265, 2009.
11. **Debacq-Chainiaux F, Erusalimsky JD, Campisi J, and Toussaint O**. Protocols to detect senescence-associated beta-galactosidase (SA-betagal) activity, a biomarker of senescent cells in culture and in vivo. *Nat Protoc* 4: 1798-1806, 2009.
12. **El Agha E, Herold S, Al Alam D, Quantius J, MacKenzie B, Carraro G, Moiseenko A, Chao CM, Minoo P, Seeger W, and Bellusci S**. Fgf10-positive cells represent a progenitor cell population during lung development and postnatally. *Development* 141: 296-306, 2014.
13. **Fernandez IE, and Eickelberg O**. New cellular and molecular mechanisms of lung injury and fibrosis in idiopathic pulmonary fibrosis. *Lancet* 380: 680-688, 2012.
14. **Fujino N, Kubo H, Suzuki T, Ota C, Hegab AE, He M, Suzuki S, Suzuki T, Yamada M, and Kondo T**. Isolation of alveolar epithelial type II progenitor cells from adult human lungs. *Laboratory investigation; a journal of technical methods and pathology* 91: 363, 2011.
15. **Ghatak S, Hascall VC, Markwald RR, Feghali-Bostwick C, Artlett CM, Gooz M, Bogatkevich GS, Atanelishvili I, Silver RM, Wood J, Thannickal VJ, and Misra S**. Transforming growth factor beta1 (TGFbeta1)-induced CD44V6-NOX4 signaling in pathogenesis of idiopathic pulmonary fibrosis. *J Biol Chem* 292: 10490-10519, 2017.
16. **Hagood JS, Prabhakaran P, Kumbla P, Salazar L, MacEwen MW, Barker TH, Ortiz LA, Schoeb T, Siegal GP, Alexander CB, Pardo A, and Selman M**. Loss of fibroblast Thy-1 expression correlates with lung fibrogenesis. *Am J Pathol* 167: 365-379, 2005.
17. **Halfon S, Abramov N, Grinblat B, and Ginis I**. Markers distinguishing mesenchymal stem cells from fibroblasts are downregulated with passaging. *Stem Cells Dev* 20: 53-66, 2011.

18. **Han X, Wang R, Zhou Y, Fei L, Sun H, Lai S, Saadatpour A, Zhou Z, Chen H, Ye F, Huang D, Xu Y, Huang W, Jiang M, Jiang X, Mao J, Chen Y, Lu C, Xie J, Fang Q, Wang Y, Yue R, Li T, Huang H, Orkin SH, Yuan GC, Chen M, and Guo G**. Mapping the Mouse Cell Atlas by Microwell-Seq. *Cell* 172: 1091-1107 e1017, 2018.

19. **Heinzelmann K, Noskovicova N, Merl-Pham J, Preissler G, Winter H, Lindner M, Hatz R, Hauck SM, Behr J, and Eickelberg O**. Surface proteome analysis identifies platelet derived growth factor receptor-alpha as a critical mediator of transforming growth factor-beta-induced collagen secretion. *Int J Biochem Cell Biol* 74: 44-59, 2016.

20. **Hinz B, Phan SH, Thannickal VJ, Galli A, Bochaton-Piallat ML, and Gabbiani G**. The myofibroblast: one function, multiple origins. *Am J Pathol* 170: 1807-1816, 2007.

21. **Horowitz JC, Ajayi IO, Kulasekaran P, Rogers DS, White JB, Townsend SK, White ES, Nho RS, Higgins PD, and Huang SK**. Survivin expression induced by endothelin-1 promotes myofibroblast resistance to apoptosis. *The international journal of biochemistry & cell biology* 44: 158-169, 2012.

22. **Horowitz JC, and Thannickal VJ**. Epithelial-mesenchymal interactions in pulmonary fibrosis. In: *Seminars in respiratory and critical care medicine*Copyright© 2006 by Thieme Medical Publishers, Inc., 333 Seventh Avenue, New York, NY 10001, USA., 2006, p. 600-612.

23. **Hostettler KE, Zhong J, Papakonstantinou E, Karakiulakis G, Tamm M, Seidel P, Sun Q, Mandal J, Lardinois D, Lambers C, and Roth M**. Anti-fibrotic effects of nintedanib in lung fibroblasts derived from patients with idiopathic pulmonary fibrosis. *Respir Res* 15: 157, 2014.

24. **Kalluri R, and Zeisberg M**. Fibroblasts in cancer. *Nat Rev Cancer* 6: 392-401, 2006.

25. **Kendall RT, and Feghali-Bostwick CA**. Fibroblasts in fibrosis: novel roles and mediators. *Front Pharmacol* 5: 123, 2014.

26. **Khanna P, Chung CY, Neves RI, Robertson GP, and Dong C**. CD82/KAI expression prevents IL-8-mediated endothelial gap formation in late-stage melanomas. *Oncogene* 33: 2898-2908, 2014.

27. **Kim KK, Sisson TH, and Horowitz JC**. Fibroblast growth factors and pulmonary fibrosis: it's more complex than it sounds. *The Journal of pathology* 241: 6-9, 2017.

28. **Kim SH, Turnbull J, and Guimond S**. Extracellular matrix and cell signalling: the dynamic cooperation of integrin, proteoglycan and growth factor receptor. *J Endocrinol* 209: 139-151, 2011.

29. **Kuilman T, Michaloglou C, Mooi WJ, and Peeper DS**. The essence of senescence. *Genes Dev* 24: 2463-2479, 2010.

30. **Kumar ME, Bogard PE, Espinoza FH, Menke DB, Kingsley DM, and Krasnow MA**. Mesenchymal cells. Defining a mesenchymal progenitor niche at single-cell resolution. *Science* 346: 1258810, 2014.

31. **Kundrotas G**. Surface markers distinguishing mesenchymal stem cells from fibroblasts. *Acta Medica Lituanica* 19: 2012.

32. **Kurundkar AR, Kurundkar D, Rangarajan S, Locy ML, Zhou Y, Liu RM, Zmijewski J, and Thannickal VJ**. The matricellular protein CCN1 enhances TGF-beta1/SMAD3-dependent profibrotic signaling in fibroblasts and contributes to fibrogenic responses to lung injury. *FASEB J* 30: 2135-2150, 2016.

33. **Lee JH, Tammela T, Hofree M, Choi J, Marjanovic ND, Han S, Canner D, Wu K, Paschini M, Bhang DH, Jacks T, Regev A, and Kim CF**. Anatomically and Functionally Distinct Lung Mesenchymal Populations Marked by Lgr5 and Lgr6. *Cell* 170: 1149-1163 e1112, 2017.

34. **Lehmann M, Baarsma HA, and Königshoff M**. WNT Signaling in Lung Aging and Disease. *Annals of the American Thoracic Society* 13: S411-S416, 2016.

35. **Lehmann M, Korfei M, Mutze K, Klee S, Skronska-Wasek W, Alsafadi HN, Ota C, Costa R, Schiller HB, Lindner M, Wagner DE, Gunther A, and Konigshoff M**. Senolytic drugs target alveolar epithelial cell function and attenuate experimental lung fibrosis ex vivo. *Eur Respir J* 50: 2017.

36. **Liu X, Wong SS, Taype CA, Kim J, Shentu TP, Espinoza CR, Finley JC, Bradley JE, Head BP, Patel HH, Mah EJ, and Hagood JS**. Thy-1 interaction with Fas in lipid rafts regulates fibroblast apoptosis and lung injury resolution. *Lab Invest* 97: 256-267, 2017.

37. **Lizardo DY, Lin YL, Gokcumen O, and Atilla-Gokcumen GE**. Regulation of lipids is central to replicative senescence. *Mol Biosyst* 13: 498-509, 2017.
38. **Lupatov AY, Vdovin AS, Vakhrushev IV, Poltavtseva RA, and Yarygin KN**. Comparative analysis of the expression of surface markers on fibroblasts and fibroblast-like cells isolated from different human tissues. *Bull Exp Biol Med* 158: 537-543, 2015.
39. **Mise N, Savai R, Yu H, Schwarz J, Kaminski N, and Eickelberg O**. Zyxin is a transforming growth factor-beta (TGF-beta)/Smad3 target gene that regulates lung cancer cell motility via integrin alpha5beta1. *J Biol Chem* 287: 31393-31405, 2012.
40. **Moore MW, and Herzog EL**. Regulation and Relevance of Myofibroblast Responses in Idiopathic Pulmonary Fibrosis. *Curr Pathobiol Rep* 1: 199-208, 2013.
41. **Munoz-Espin D, and Serrano M**. Cellular senescence: from physiology to pathology. *Nat Rev Mol Cell Biol* 15: 482-496, 2014.
42. **Niehage C, Steenblock C, Pursche T, Bornhauser M, Corbeil D, and Hoflack B**. The cell surface proteome of human mesenchymal stromal cells. *PLoS One* 6: e20399, 2011.
43. **O'Dwyer DN, Ashley SL, and Moore BB**. Influences of innate immunity, autophagy, and fibroblast activation in the pathogenesis of lung fibrosis. *Am J Physiol Lung Cell Mol Physiol* 311: L590-601, 2016.
44. **Park YM**. CD36, a scavenger receptor implicated in atherosclerosis. *Exp Mol Med* 46: e99, 2014.
45. **Parks BW, Black LL, Zimmerman KA, Metz AE, Steele C, Murphy-Ullrich JE, and Kabarowski JH**. CD36, but not G2A, modulates efferocytosis, inflammation, and fibrosis following bleomycin-induced lung injury. *J Lipid Res* 54: 1114-1123, 2013.
46. **Phan SH**. Biology of fibroblasts and myofibroblasts. *Proc Am Thorac Soc* 5: 334-337, 2008.
47. **Pilling D, Fan T, Huang D, Kaul B, and Gomer RH**. Identification of markers that distinguish monocyte-derived fibrocytes from monocytes, macrophages, and fibroblasts. *PLoS One* 4: e7475, 2009.
48. **Raghu G, Collard HR, Egan JJ, Martinez FJ, Behr J, Brown KK, Colby TV, Cordier JF, Flaherty KR, Lasky JA, Lynch DA, Ryu JH, Swigris JJ, Wells AU, Ancochea J, Bouros D, Carvalho C, Costabel U, Ebina M, Hansell DM, Johkoh T, Kim DS, King TE, Jr., Kondoh Y, Myers J, Muller NL, Nicholson AG, Richeldi L, Selman M, Dudden RF, Griss BS, Protzko SL, Schunemann HJ, and Fibrosis AEJACoIP**. An official ATS/ERS/JRS/ALAT statement: idiopathic pulmonary fibrosis: evidence-based guidelines for diagnosis and management. *Am J Respir Crit Care Med* 183: 788-824, 2011.
49. **Ramirez G, Hagood JS, Sanders Y, Ramirez R, Becerril C, Segura L, Barrera L, Selman M, and Pardo A**. Absence of Thy-1 results in TGF-beta induced MMP-9 expression and confers a profibrotic phenotype to human lung fibroblasts. *Lab Invest* 91: 1206-1218, 2011.
50. **Ridge KM, Shumaker D, Robert A, Hookway C, Gelfand VI, Janmey PA, Lowery J, Guo M, Weitz DA, and Kuczmarski E**. Methods for Determining the Cellular Functions of Vimentin Intermediate Filaments. *Methods in Enzymology* 568: 389-426, 2016.
51. **Ruiz-Camp J, and Morty RE**. Divergent fibroblast growth factor signaling pathways in lung fibroblast subsets: where do we go from here? *Am J Physiol Lung Cell Mol Physiol* 309: L751-755, 2015.
52. **Sakai N, Chun J, Duffield JS, Wada T, Luster AD, and Tager AM**. LPA1-induced cytoskeleton reorganization drives fibrosis through CTGF-dependent fibroblast proliferation. *The FASEB Journal* 27: 1830-1846, 2013.
53. **Sakai N, and Tager AM**. Fibrosis of two: Epithelial cell-fibroblast interactions in pulmonary fibrosis. *Biochimica et Biophysica Acta (BBA)-Molecular Basis of Disease* 1832: 911-921, 2013.
54. **Sanders YY, Pardo A, Selman M, Nuovo GJ, Tollefsbol TO, Siegal GP, and Hagood JS**. Thy-1 promoter hypermethylation: a novel epigenetic pathogenic mechanism in pulmonary fibrosis. *Am J Respir Cell Mol Biol* 39: 610-618, 2008.
55. **Schafer MJ, White TA, Iijima K, Haak AJ, Ligresti G, Atkinson EJ, Oberg AL, Birch J, Salmonowicz H, Zhu Y, Mazula DL, Brooks RW, Fuhrmann-Stroissnigg H, Pirtskhalava T, Prakash YS,**

Tchkonia T, Robbins PD, Aubry MC, Passos JF, Kirkland JL, Tschumperlin DJ, Kita H, and LeBrasseur NK. Cellular senescence mediates fibrotic pulmonary disease. *Nat Commun* 8: 14532, 2017.

56. **Seluanov A, Vaidya A, and Gorbunova V**. Establishing primary adult fibroblast cultures from rodents. *J Vis Exp* 2010.

57. **Staab-Weijnitz CA, Fernandez IE, Knuppel L, Maul J, Heinzelmann K, Juan-Guardela BM, Hennen E, Preissler G, Winter H, Neurohr C, Hatz R, Lindner M, Behr J, Kaminski N, and Eickelberg O**. FK506-Binding Protein 10, a Potential Novel Drug Target for Idiopathic Pulmonary Fibrosis. *Am J Respir Crit Care Med* 192: 455-467, 2015.

58. **Takashima A**. Establishment of fibroblast cultures. *Curr Protoc Cell Biol* Chapter 2: Unit 2 1, 2001.

59. **Tamm M, Roth M, Malouf M, Chhajed P, Johnson P, Black J, and Glanville A**. Primary fibroblast cell cultures from transbronchial biopsies of lung transplant recipients. *Transplantation* 71: 337-339, 2001.

60. **Walmsley GG, Rinkevich Y, Hu MS, Montoro DT, Lo DD, McArdle A, Maan ZN, Morrison SD, Duscher D, Whittam AJ, Wong VW, Weissman IL, Gurtner GC, and Longaker MT**. Live fibroblast harvest reveals surface marker shift in vitro. *Tissue Eng Part C Methods* 21: 314-321, 2015.

61. **Wang R, Ramos C, Joshi I, Zagariya A, Pardo A, Selman M, and Uhal BD**. Human lung myofibroblast-derived inducers of alveolar epithelial apoptosis identified as angiotensin peptides. *Am J Physiol* 277: L1158-1164, 1999.

62. **Wang T, Ward Y, Tian L, Lake R, Guedez L, Stetler-Stevenson WG, and Kelly K**. CD97, an adhesion receptor on inflammatory cells, stimulates angiogenesis through binding integrin counterreceptors on endothelial cells. *Blood* 105: 2836-2844, 2005.

63. **Wang X, Chen Y, Lv L, and Chen J**. Silencing CD36 gene expression results in the inhibition of latent-TGF-beta1 activation and suppression of silica-induced lung fibrosis in the rat. *Respir Res* 10: 36, 2009.

64. **Waters DW, Blokland KEC, Pathinayake PS, Burgess JK, Mutsaers SE, Prele CM, Schuliga M, Grainge CL, and Knight DA**. Fibroblast senescence in the pathology of idiopathic pulmonary fibrosis. *Am J Physiol Lung Cell Mol Physiol* 2018.

65. **Wyman AE, Noor Z, Fishelevich R, Lockatell V, Shah NG, Todd NW, and Atamas SP**. Sirtuin 7 is decreased in pulmonary fibrosis and regulates the fibrotic phenotype of lung fibroblasts. *Am J Physiol Lung Cell Mol Physiol* 312: L945-L958, 2017.

66. **Xie T, Wang Y, Deng N, Huang G, Taghavifar F, Geng Y, Liu N, Kulur V, Yao C, Chen P, Liu Z, Stripp B, Tang J, Liang J, Noble PW, and Jiang D**. Single-Cell Deconvolution of Fibroblast Heterogeneity in Mouse Pulmonary Fibrosis. *Cell Rep* 22: 3625-3640, 2018.

67. **Yoon IK, Kim HK, Kim YK, Song IH, Kim W, Kim S, Baek SH, Kim JH, and Kim JR**. Exploration of replicative senescence-associated genes in human dermal fibroblasts by cDNA microarray technology. *Exp Gerontol* 39: 1369-1378, 2004.

Figure Captions

Figure 1. Heterogeneous expression pattern of mesenchymal markers in primary lung fibroblasts. A,B) For immunofluorescent stainings, primary human lung fibroblasts passage 4-5 were seeded in a 96-well Imagerplate, fixed the next day with 4% PFA and single (A) or double stained (B) with primary antibodies as indicated and further incubated with secondary antibodies conjugated to Alexa fluor-488 (green) or -568 (red). Nuclei were stained by DAPI (blue). Shown is one representative experiment of 5-6 independent experiments. Single positive cells in (B) are highlighted by a white arrow. Bar size: left picture 50 µm, right picture (higher magnification) 40 µm. C) The percentage of single positive cells for each marker was assessed by counting of positive and total cells (total cell number was determined by the software Imaris). Shown is a summary of 2-3 independent biological experiments consisting of 2-5 technical replicates. D) Cells double stained for different marker combinations as indicated in Fig. B were quantified by counting for marker negativity, single positivity for each marker and double positivity. Summarized are 3-4 biological experiments consisting of 2-3 technical replicates. All data are represented as ±SEM. * refers to stress fiber positive presence only.

Figure 2. Mesenchymal marker expression quantified by FACS. The number of positive cells for the indicated mesenchymal markers were determined by FACS. Dot blots and histograms of one experiment are presented in (A), with isotype controls shown in red and the positive population in blue. Summary of 11 independent FACS experiments ±SD of primary fibroblasts in passage 4 is provided in (B). One-way ANOVA followed by Tukey's multiple comparison test was performed to determine significant differences. ns = not significant.

Figure 3. Detection of tetraspanins on the surface of primary fibroblasts. Expression and surface localization of tetraspanins (previously identified by a proteome analysis) on primary lung fibroblasts (passage 4) was analyzed by FACS and one representative FACS experiment is presented in dot blots and histograms with positive populations in blue and corresponding isotype controls in red (A). The number of positive cells and the median fluorescence

intensities (ΔMFI, by subtraction of isotype MFI values) of 5-13 independent biological FACS experiments ±SD is summarized in (B) and (C).

Figure 4. Surface marker expression and localization on primary lung fibroblasts. Expression and surface localization of several surface markers (also previously identified by the proteome analysis) on primary lung fibroblasts (passage 4-5) was determined by FACS. Markers functionally and/or structurally belong to different groups of proteins and are not further subcategorized. A representative FACS experiment is presented in dot blots and histograms with positive populations in blue and corresponding isotype controls in red (A). The number of positive cells and the median fluorescence intensities (ΔMFI, by subtraction of isotype MFI values) of 5-13 independent biological FACS experiments ±SD is summarized in (B) and (C).

Figure 5. Surface marker expression over time in culture. Changes in the number of positive cells for indicated markers between passage 1 and 7 were determined by FACS. Dot blots and histograms of one representative experiment for passage 1 and 3 is provided in (A). Positive populations of CD36, CD47, CD54, CD82, CD106 and CD140a are shown in blue with corresponding isotype controls in red. A summary of 3-6 independent biological FACS experiments ±SD for all passages is shown in (B) and (C). For statistical analysis one-way ANOVA followed by Bonferroni's multiple comparison test (column comparison to passage 1) was performed. * $p<0.05$, ** $p<0.01$.

Figure 6. Replicative senescence in primary lung fibroblasts. For assessment of senescence, cells in different passages were seeded in 6-well plates and analyzed after 96 hours (A-E). Cells were stained for senescence associated β-Galactosidase activity and images were acquired with a light microscope (magnification: 100x) (A). The percentage of senescent cells was assessed by counting of positive and total cells (B). IL-6 ELISA of primary lung fibroblasts supernatant (C). Total cell number was determined by counting of cells and population

doubling times were calculated (D). Full blots of a representative Western Blot of 4 (p3-p11) independent biological experiments of P16 and P21 protein levels in primary lung fibroblasts in different passages is shown in (E); irrelevant lanes were cropped off the right side of the blot. M = protein marker. Values of (B,C,D) are given as ± SEM for an n of 3-9. Statistical significance was determined by One-way ANOVA followed by Neuman-Keuls multiple comparison test (*p<0.05; **p<0.01; ***p<0.001).

Figure 7. Subtype marker expression in differentiated myofibroblasts. A) To analyze the expression of subtype markers in differentiated myofibroblasts, fibroblasts (passage 4-5) were stimulated twice every 24 hours with 1 or 2 ng/ml TGF-β for 48 hours, stained with fluorochrome conjugated antibodies and the number of positive cells determined for indicated markers by FACS analysis. Shown are results of 5-11 independent biological FACS experiments ±SD. For statistical analysis a paired two-tailed t-test was performed. * p<0.05, ** p<0.01, ns = not significant. B-D) To analyze if CD36 and CD97 positive cells represent a senescent population of fibroblasts, cells (passage 9-10) were stimulated with bafilomycin A1 (100 nm) for 1 h, C_{12}FDG (33 µM; DMSO as control) added for further 2 h, and cells stained with CD36-APC or CD97-APC for FACS analysis. Dot blots of one experiment in the presence/absence of C_{12}FDG, read out by Alexa fluor 488, are presented in (B), with isotype controls shown in red and the positive population in blue. A summary for the senescence of cells of 7 independent FACS experiments ±SD is provided in (C). The number of CD36 and CD97 positive cells in the presence/absence of C_{12}FDG (n4-6) is summarized in (D). A paired two-tailed t-test was performed for statistical analysis. *** p<0.001, ns = not significant.

Figure 8. Subtype marker expression in human lung tissue. For immunohistochemistry of subtype markers in IPF and control, paraffin embedded lung sections of 200 µm were deparaffinized and after antigen retrieval stained with primary antibodies as indicated together with αSMA and further incubated with secondary antibodies conjugated to Alexa fluor-488 (green) or -568 (red). Nuclei were stained by DAPI (blue). Red cells indicate positive subtype markers, green cells are stained positive for αSMA. Shown is one representative

724 experiment of 3-4 independent biological experiments. A 2-fold magnification is shown for
725 representative areas indicated by a quadrangle. Bar size: 20 µm.

726

Tables

Table 1. Antibodies

Antibody	Host/Isotype	Application	Company	Catalog-no.	Dilution
PDGFRα (CD140a)-PE	mouse/IgG1	FACS	Biolegend	323505	1:5
PDGFRβ (CD140b)-PE	mouse/IgG1	FACS	Biolegend	323605	1:20
CD9-PE	mouse/IgG1	FACS	Biolegend	312105	1:100
CD26-APC	mouse/IgG2a	FACS	Biolegend	302709	1:6
CD36-PE/APC	mouse/IgG2a	FACS	Biolegend	336205/336207	1:10/1:10
CD36	rabbit/IgG	IHC-P	Abcam	ab133625	1:100
CD34-PE	mouse/IgG2a	FACS	Biolegend	343605	1:10
CD44-FITC	rat/IgG2b	FACS	ebioscience	11-0441-82	1:100
CD45-V450	mouse/IgG1	FACS	BD	560367	1:20
CD46-FITC	mouse/IgG1	FACS	Biolegend	315304	1:20
CD47-FITC	mouse/IgG1	FACS	Biolegend	323106	1:20
CD54-FITC	mouse/IgG1	FACS	Biolegend	353107	1:200
CD55-APC	mouse/IgG1	FACS	Biolegend	311311	1:1000
CD59-PE	mouse/IgG2a	FACS	Biolegend	304707	1:500
CD63-PE	mouse/IgG1	FACS	Biolegend	353003	1:25
CD73-PerCP/Cy5.5	mouse/IgG1	FACS	Biolegend	344013	1:100
CD81-FITC	mouse/IgG1	FACS	Biolegend	349503	1:20
CD82-PE	mouse/IgG1	FACS	Biolegend	342103	1:500
CD90/Thy-1-APC	mouse/IgG1	FACS	ebioscience	17-0909-42	1:200
CD97-PE/APC	mouse/IgG1	FACS	Biolegend/ eBioscience	336307/ 17-6979-42	1:10/1:10
CD97	rabbit/IgG	IHC-P	Abcam	ab108368	1:250
CD105-APC	mouse/IgG1	FACS	ebioscience	17-1057-41	1:25
CD106-APC	mouse/IgG1	FACS	Biolegend	305809	1:5
CD151 (PETA-3)-APC	mouse/IgG1	FACS	Biolegend	350405	1:100
Isotype mouse IgG1-APC	---	FACS	Biolegend	400121	---
Isotype mouse IgG1-APC	---	FACS	ebioscience	17-4714	---
Isotype mouse IgG1-PE	---	FACS	Biolegend	400113	---
Isotype mouse IgG1-FITC	---	FACS	Biolegend	400109	---
Isotype mouse IgG1-V450	---	FACS	BD	560373	---
Isotype mouse IgG2a-APC	---	FACS	Biolegend	400221	---
Isotype mouse IgG2a-PE	---	FACS	Biolegend	400211	---
Isotype mouse IgG1-PerCp/Cy5.5	---	FACS	Biolegend	400149	---
Isotype rat IgG2b-FITC	---	FACS	ebioscience	11-4031-81	---
Desmin (Y-20)	goat/IgG	IF/IHC-P	Santa Cruz	sc-7559	1:200/1:200
CD90/Thy-1	mouse/IgG2a	IF	ebioscience	14-9090-82	1:500
Collagen type I	rabbit/IgG	IF/IHC-P	Rockland	600-401-103-0.5	1:1000/1:200
Fibronectin (H-300)	rabbit/IgG	IF/IHC-P	Santa Cruz	sc-9068	1:200/1:200
αSMA	mouse	IF/IHC-P	Sigma-Aldrich	A5228	1:2000/1:5000
P16 (p16INK4a/CDKN2A)	goat/IgG	WB	R&D	AF5779	1:1000
P21	mouse/IgG	WB	Chemicon	MAB88058	1:1000
Beta-Actin	HRP-conjugated mouse	WB	Sigma-Aldrich	A3854-200UL	1:25000
HRP linked mouse IgG	---	WB	GE Healthcare	NA931-1ml	1:25000

HRP rabbit anti goat IgG	---	WB	Invitrogen	61-1620	1:25000
Donkey-anti-rabbit Alexa fluor 488/568	donkey	IF/IHC-P	Invitrogen	A-21206/ A10042	1:250/1:250
Donkey-anti-goat-Alexa fluor 488/568	donkey	IF/IHC-P	Invitrogen	A-11055	1:250/1:250
Donkey-anti-mouse Alexa fluor 488	donkey	IF/IHC-P	Invitrogen	A-21202	1:250

729

730 Table 2. IPF patient demographics and clinical information

IPF subjects	5
Age (years)	60 (±7)
Sex	
Male	5 (100%)
Female	0 (0%)
Smoking status	
Current	0 (0%)
Former	4 (80%)
Nonsmoker	0 (0%)
D_{LCO} % pred	19.5 (±4.9) (n2)
FVC % pred	39.8 (±11.4)

731

732

Figure 1. Heterogeneous expression pattern of mesenchymal markers in primary lung fibroblasts.

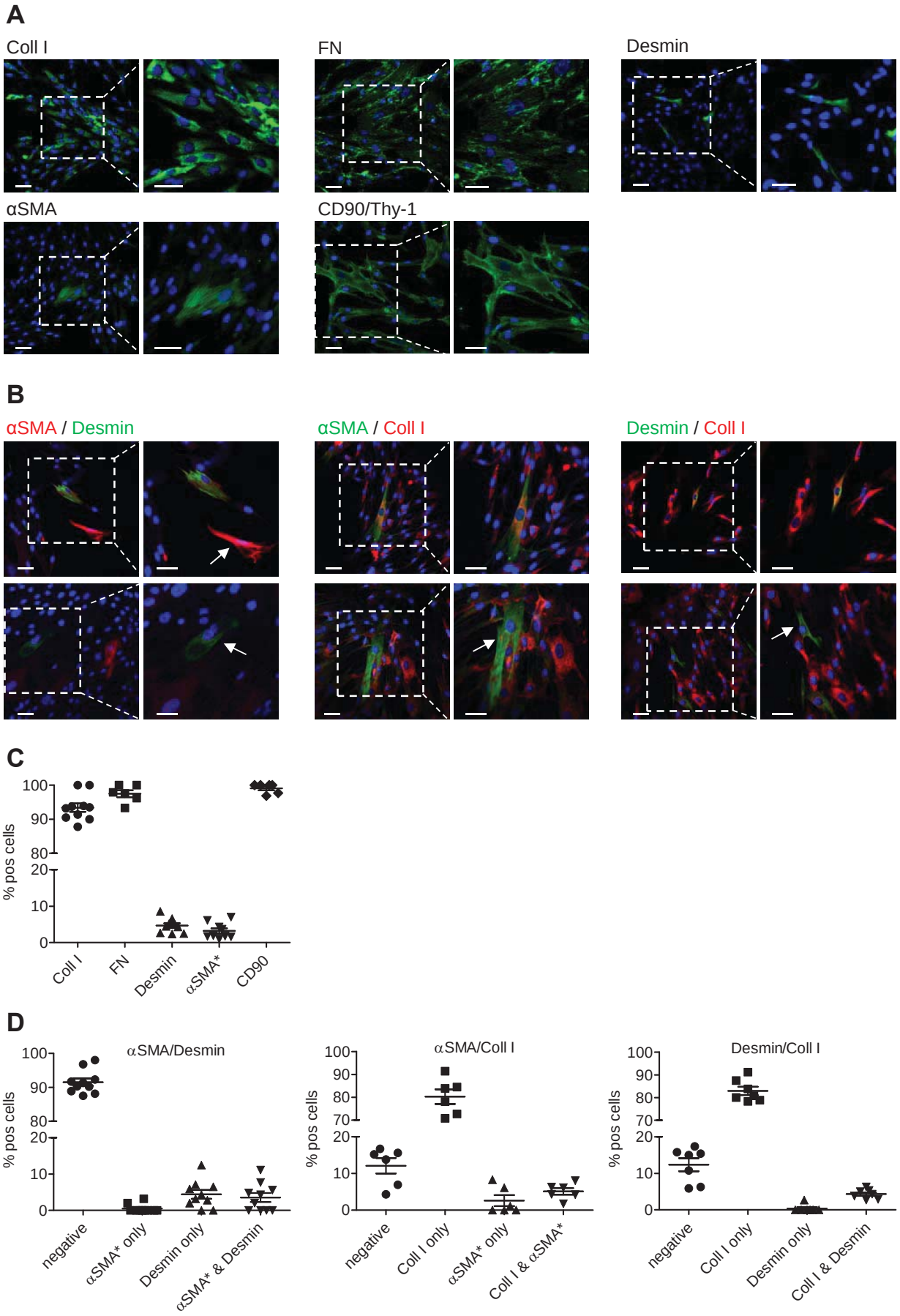

Figure 2. Mesenchymal marker expression quantified by FACS.

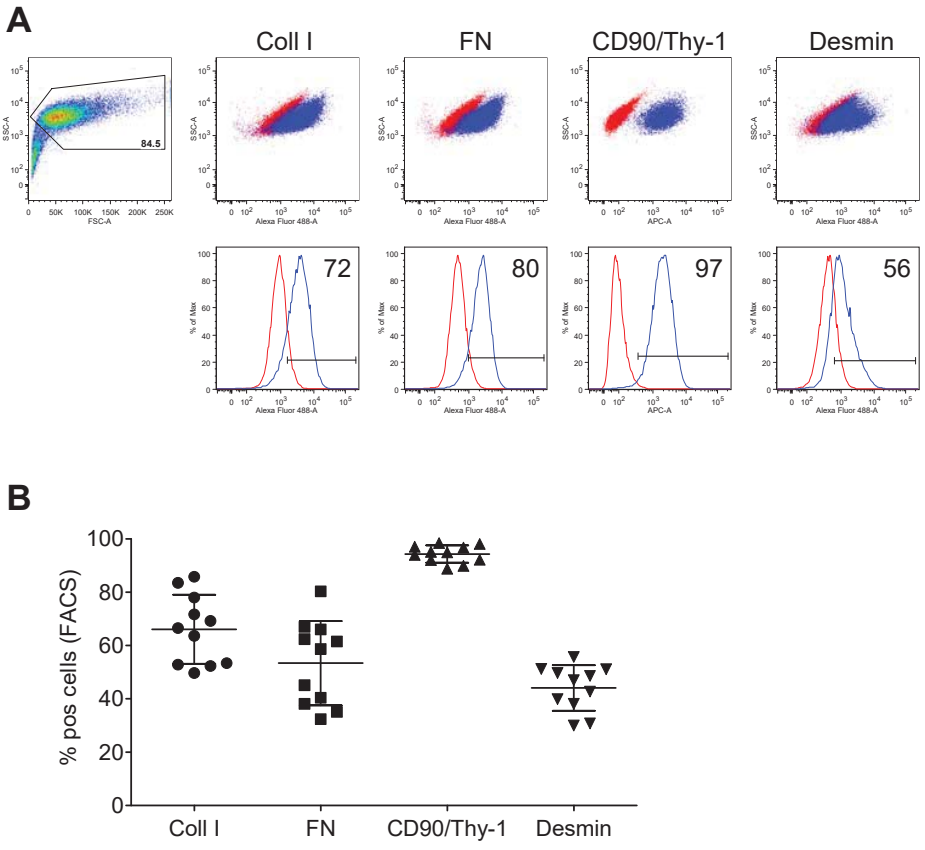

Figure 3. Detection of tetraspanins on the surface of primary fibroblasts.

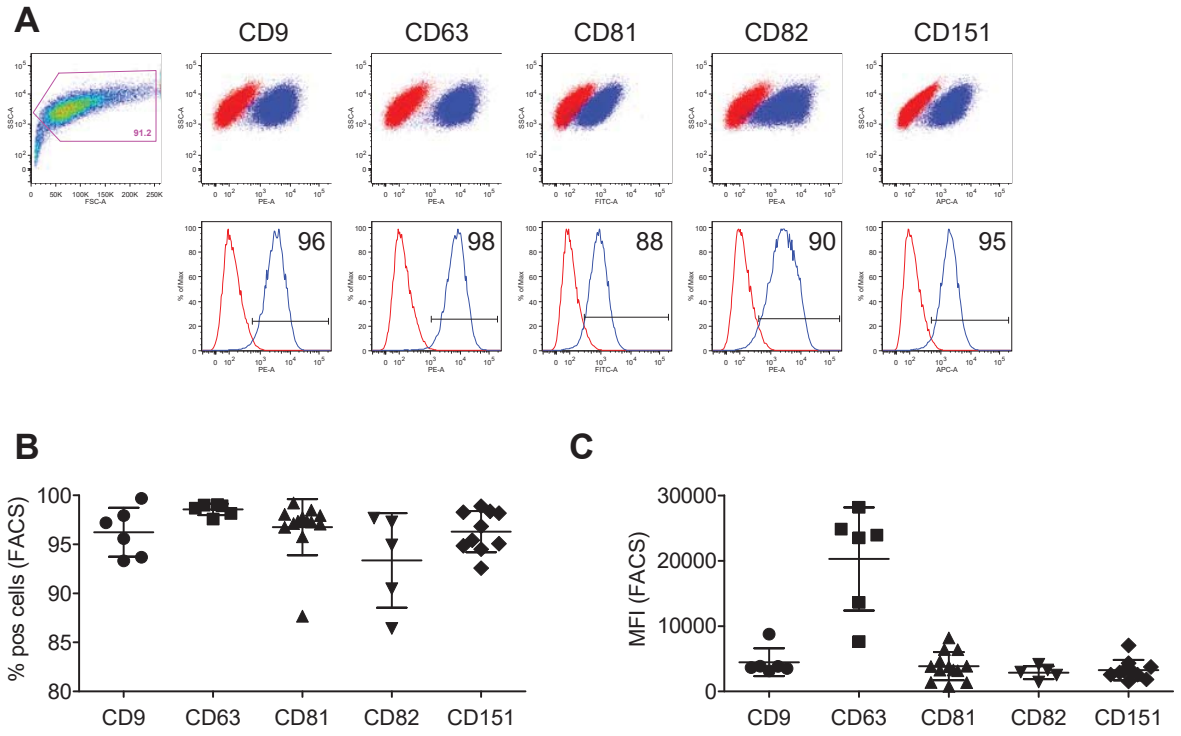

Figure 4. Surface marker expression and localization on primary lung fibroblasts.

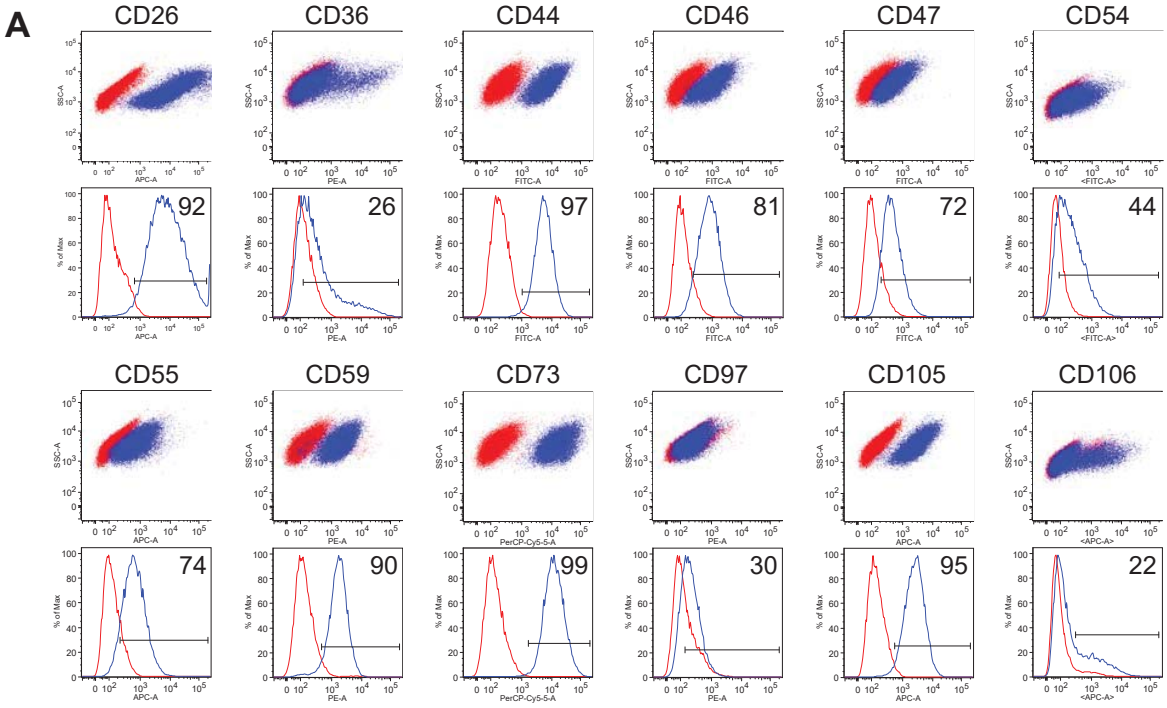

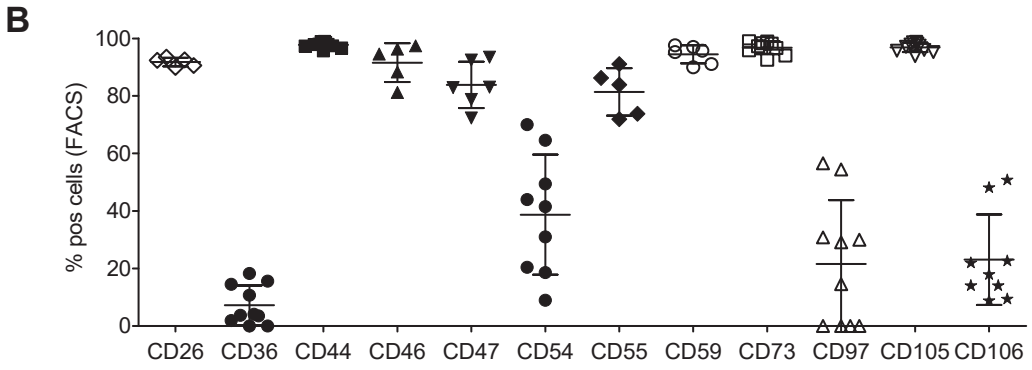

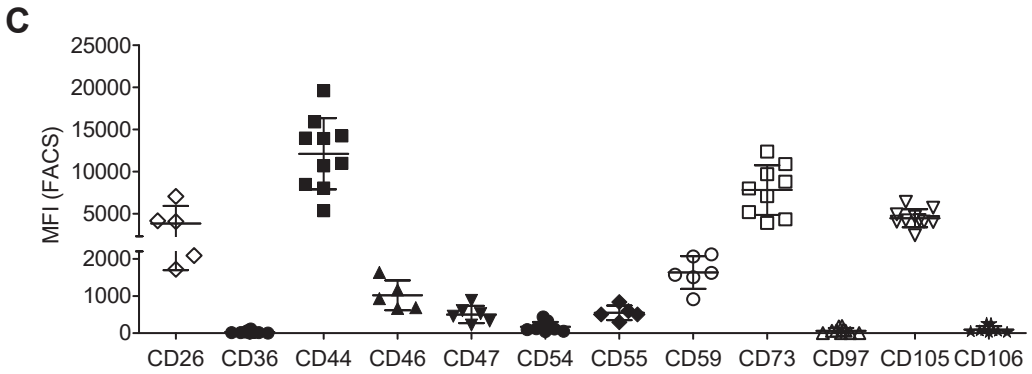

Figure 5. Surface marker expression over time in culture.

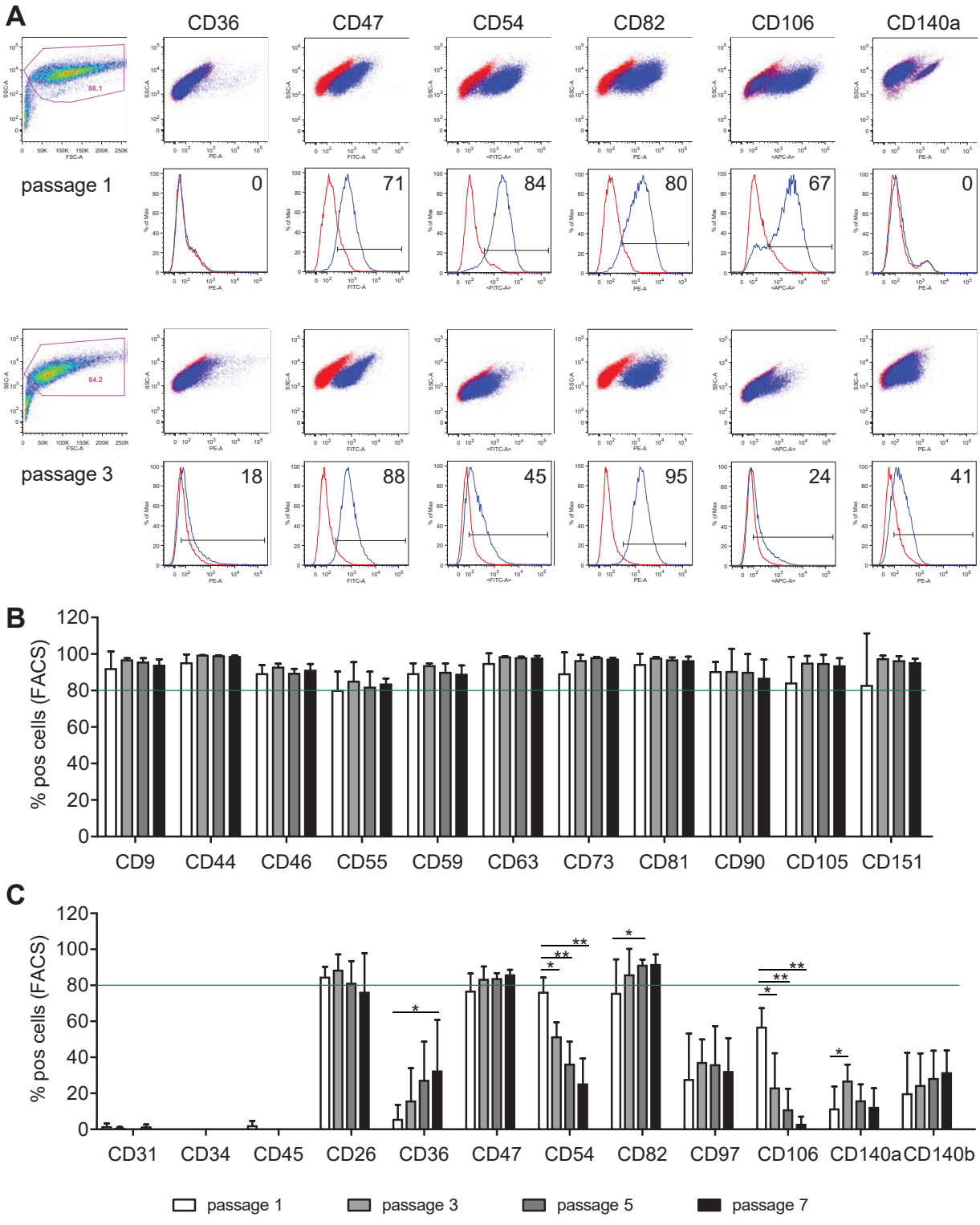

Figure 6. Replicative senescence in primary lung fibroblasts.

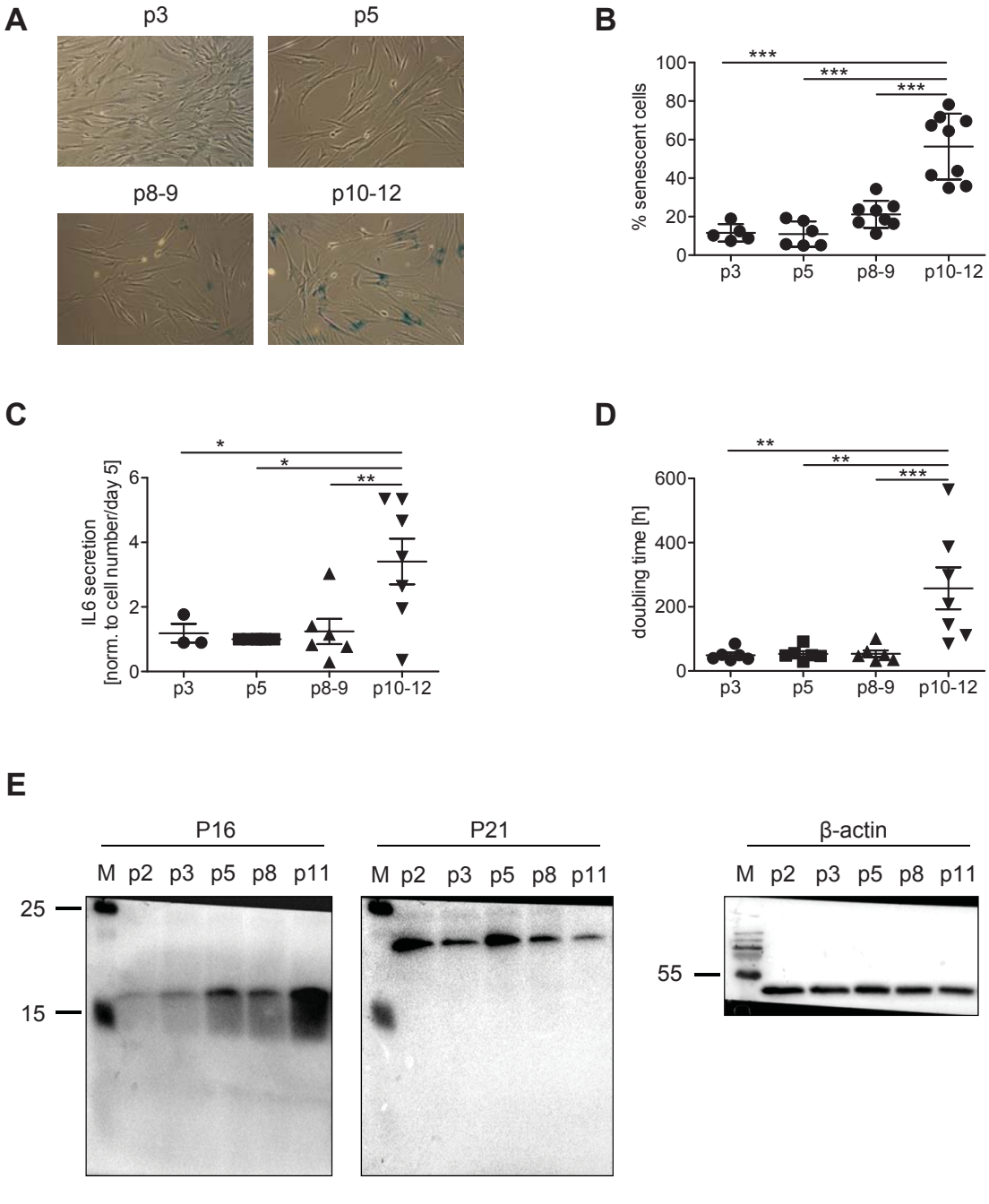

Figure 7. Quantification of subtype marker expression in differentiated myofibroblasts.

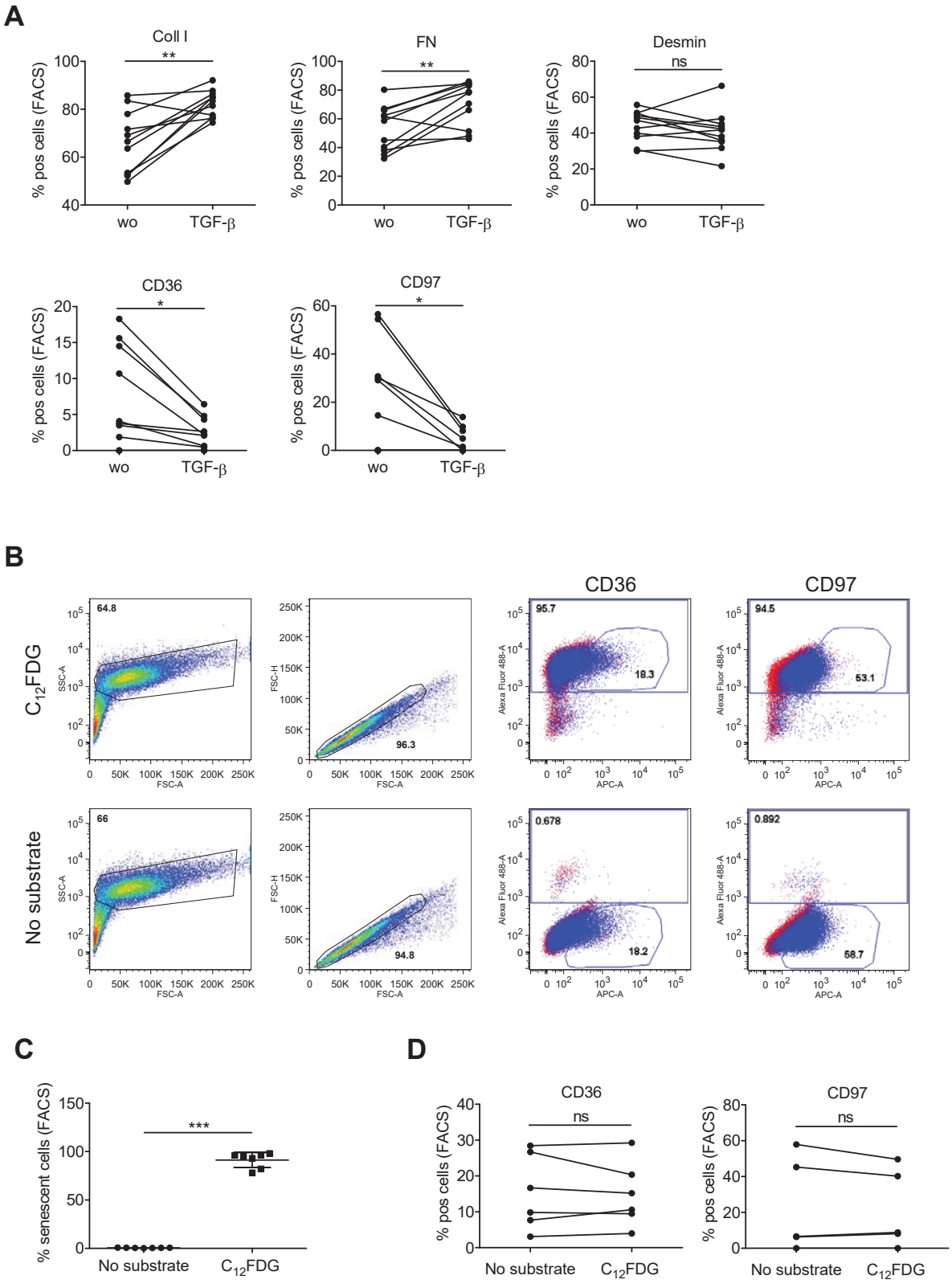

Figure 8. Subtype marker expression in human lung tissue.